



## ERROR ESTIMATION AND ADAPTIVITY FOR A MIXED FORMULATION OF LIMIT ANALYSIS

Cyntia Gonçalves da Costa  
Lavinia Sanabio Alves Borges  
Nestor Zouain

Universidade Federal do Rio de Janeiro, COPPE/EE  
Department of Mechanical Engineering  
P.O. Box 68503 — 21945-970 — Rio de Janeiro, RJ, Brazil.

Raul Antonino Feijóo  
LNCC - Laboratório Nacional de Computação Científica.  
Department of Computational Mechanical  
Rua Getúlio Vargas, 333 — 25651-070 — Petrópolis, RJ, Brazil.

**Abstract.** *The main objective of this paper is to propose an adaptive mesh refinement process for mixed finite element models in limit analysis. We use an 'a posteriori' error estimator based on a local directional interpolation error and a recovering procedure for the second derivatives of the finite element solution. The mesh adaptation process proposed gives improved results in localizing regions of rapid or abrupt variations of the variables, whose location are not known a priori. We apply the above procedure to limit analysis considering bodies in plane strain and with symmetry of revolution.*

**Keywords:** *Finite Elements, Mesh Generation, Error Estimator, Adaptive Analysis, Limit Analysis.*

### 1. INTRODUCTION

The main objective of this paper is to propose an adaptive mesh refinement process for limit analysis, using a *a posteriori* error estimator based on the local directional interpolation error and a recovering procedure for the second derivatives of the finite element solution. The strategy presented herein is an extent of the one presented by Borges *et al.*(1998) and Feijóo *et al.*(1997) where the error estimator and the adaptive process were only defined for linear finite elements. We generalize the error estimator and the adaptive procedure to include quadratic triangles.

The goal of the anisotropic mesh adaptation process, generated by a directional error

estimator, is to achieve a mesh-adaptive strategy accounting for mesh size refinement, as well as redefinition of the oriented element stretching. In this way, along the adaptation process, the mesh turns aligned with the direction of maximum curvature of the function. This mesh adaptation process gives improved results in localizing regions of rapid or abrupt variations of the variables, whose location is not known *a priori* (Peiró,1989). So, we can obtain an accurate representation of shocks, boundary layers, wakes and other discontinuities.

Limit analysis deals with the direct computation of the load producing plastic collapse of a body - a phenomenon where, under constant stresses, kinematically admissible plastic strain rates take place. Localized plastic deformations or slip bands are present in most collapse situations. Accuracy in the numerical solution of limit analysis is seriously affected by local singularities arising from these localized plastic deformations. In limit analysis, *a priori* error estimate, as provided by the standard error analysis in the finite element method, is often insufficient to assure reliable estimates of the computed solution accuracy. This is due to the fact that it only yields information on the asymptotic error behaviour and requires regularity conditions of the solution, which are not satisfied in the presence of singularities such as the above mentioned ones. Those facts disclose the need of an estimator which can *a posteriori* be extracted from the numerical solution.

Furthermore, for limit analysis, the classical three-node finite element, that use linear interpolant for the velocity field, has strong tendency to lock, so that we only use it in plane stress problems. The locking characteristics are important in plane strain and in solids with symmetry of revolution. This is because the exact velocity is an isocoric field when the Mises plastic function is used. In these cases, a curved triangular mixed element was specially created to face the lock problem (Borges *et al.*,1996). For this element an efficient adaptive strategy demands an error not necessarily piecewise constant by element, just as was previously proposed.

In this paper, firstly, we discuss some issues of the adopted error estimation techniques, by considering the derivatives recovery and the proposal directional error estimator. Following, we present the theoretical framework of limit analysis. Together with limit analysis applications, we also present an adaptive mesh refinement solution for an interpolation problem in order to show that the proposed adaptive strategy using our anisotropic error estimator recovers optimal and/or superconvergence rates.

## 2. ESTIMATORS BASED ON DERIVATIVES RECOVERY

In recovery based on error estimation methods the gradients and/or Hessians of solutions, obtained on a given mesh, are smoothed and after that the smoothed solution is used in error estimation. It is well known that the derivatives of the  $u_h$  function is superconvergent in some interior points of the mesh elements, that is, in these points the derivatives of the finite element solutions exhibit higher accuracy than normally expected. Taking advantage of superconvergent, the main idea of the proposed estimator is focused on the recovering of the Hessian with a higher order of accuracy than that naturally obtained from the finite element approximation. So, in order to obtain the proposed error estimator, it is necessary to recover the Hessian matrix from the information given by the finite element solution itself  $u_h$ . Almost every algorithm to recovering the Hessian matrix use first derivatives information. Recovering first and second derivatives are main issues of the following sections.

## 2.1. The interpolation error as an indicator of the approximate solution

We present an anisotropic posteriori error estimator for the difference between a given function  $u$  and a discrete function  $U \in V_h$  which is a good approximation of  $u$  in  $\Omega$  in the sense that

$$\|u - U\|_{L^p(\Omega)} \leq C \|u - \Pi u\|_{L^p(\Omega)} \quad (1)$$

with  $\Pi : W^{2,p}(\Omega) \rightarrow V_h$  denoting an operator whose approximation properties are similar to the Clément interpolation. Based on Eq.(1) and in accordance with Almeida *et al.*,(1998), we assume that exists a constant  $C$  such that

$$\|u - u_h\|_{L^p(\Omega)} \simeq C \|\mathcal{H}_R(u_h(x))(x - x_0) \cdot (x - x_0)\|_{L^p(\Omega)} \quad (2)$$

where  $\mathcal{H}_R(u_h(x))$  denotes the recovered Hessian matrix obtained from the information given by the finite element solution  $u_h$ . This shows that the interpolation error in one point  $x$ , where  $|x - x_0|$  is small enough, is governed by the behaviour of the second order derivative in such point. Thus the interpolation error is not distributed in an isotropic way around the point  $x_0$ , i.e., the error depends on the direction  $x - x_0$  and the recovered Hessian matrix value in this point,  $\mathcal{H}_R(u(x))$ .

The above result suggests the use of Eq.(2) as a *directional* error estimator in the terminology used by Peiró (1989). Since the recovered Hessian matrix is not positive definite it can not be taken as a metric tensor. As an alternative, Peiró introduced the metric tensor

$$\mathbf{G} = \mathbf{Q}\mathbf{\Lambda}\mathbf{Q}^T \quad (3)$$

where  $\mathbf{Q}$  is the matrix of eigenvectors of the recovered Hessian matrix, the matrix  $\mathbf{\Lambda} = \text{diag}\{|\lambda_1|, |\lambda_2|\}$  and  $|\lambda_i|, i = 1, 2$ , are the absolute value of the associated eigenvalues ( $|\lambda_1| \leq |\lambda_2|$ ). According to this definition, the metric tensor field  $\mathbf{G}$  is at least positive semi-definite. In particular, a zero eigenvalue poses no difficulty since it leads to infinite mesh sizes that are inhibited by the element size limitation or by the finiteness of the computational domain.

The error estimator introduced herein, instead of considering an error estimator associated to the element edge length, as proposed by Dompierre *et al.*, (1995), uses another one that provides a measure of the second derivative contribution in each element. Considering a given finite element mesh  $\mathfrak{S}$  of the domain  $\Omega$ , the error estimator at element level  $T \in \mathfrak{S}$ , is defined by the expression

$$\eta_T = \left\{ \int_{\Omega_T} [\mathbf{G}(u_h(x_0))(x - x_0) \cdot (x - x_0)]^p d\Omega \right\}^{\frac{1}{p}} \quad (4)$$

where  $\Omega_T$  is the area of the element  $T$  and  $x_0$  is the center of this element. The global error estimator  $\eta$  is given by:

$$\eta = \left( \sum_{T \in \mathfrak{S}} \eta_T^p \right)^{\frac{1}{p}} \quad (5)$$

## 2.2. First order derivative recuperation

Several approaches have been proposed, in the framework of the Finite Element Method, in order to recover first derivatives (see for example Zienkiewicz & Zhu,1992). Among them there is the Weighted Average which we briefly summarize.

The approach quoted Weight Average consists on turning the inter-elements discontinuous field  $\nabla u_h$  into the continuous field  $\nabla_R u_h$ . This is made by employing the same element basis functions used to construct  $u_h$  to compute  $\nabla u_h$ , and then adopting a weighted average of the  $\nabla u_h$ , computed on the elements surrounding a node  $N$ , as the value  $\nabla_R u_h(\mathbf{X}_N)$  of the recovered gradient in this node ( $\mathbf{X}_N$  is the coordinate of node  $N$ ). The weight average is computed using weights given by the inverse of the distance between the node  $N$  and the points of superconvergence of the gradient (the center of the element in the case of linear triangles and the gauss point near midside nodes in the case of quadratic triangles (Zienkiewicz& Zhu,1992)). The weights can also be defined by the area of the elements surrounding the node.

Second derivatives can also be recovered by using the same approaches used for the first derivative recuperation. In fact, taking  $\nabla_R u_h$  as a new field, we can reapply the algorithm in order to find  $\nabla_R(\nabla_R u_h)$ . The symmetric part of the approximation is retained in order to ensure the symmetry of recovered Hessian matrix.

In order to approximate functions presenting strong variations in the derivatives the adapted mesh turns to be oriented by means of the stretching of its elements in the direction of maximum curvature of the function. Whenever this stretching is very large may cause poor precision when computing weighted averages. To overcome this situation, the original domain  $\Omega_T$  is locally transformed into a standard unstretched domain  $\Omega_T^*$ . For instance, when using mesh generators based on the *advancing front technique* (Fancello *et al*,1990) this domain transformation is naturally choosed compatible with the domain mapping which is part of the mesh generation algorithm. This is the procedure adopted in the present work and is described in the following.

Considering the neighborhood of an arbitrary point  $N$ , the mesh generation algorithm tends to create triangular elements which are equilateral when viewed in the transformed domain given by the following operator:

$$\mathbf{S}(N) = \frac{1}{s(N) * h(N)} \mathbf{e}_1 \otimes \mathbf{e}_1 + \frac{1}{h(N)} \mathbf{e}_2 \otimes \mathbf{e}_2 \quad (6)$$

where  $\mathbf{e}_i(N), i = 1, 2$  are the eigenvectors of the Hessian matrix  $\mathbf{H}(u_h(N))$ ,  $h(N)$  is the size in the  $\mathbf{e}_2$  direction and  $s \geq 1$  is the stretching in the  $\mathbf{e}_1$  direction of an element generated at node  $N$ . Those parameters are all dynamically defined along the mesh adaptation process. The selection of these parameters is discussed in the next section.

Consequently, each point  $M$  belonging to some element adjacent to a node  $N$  of the mesh mapped in a point  $\mathbf{x}_M$  given by:

$$\mathbf{x}_M = \mathbf{S}(N)(\mathbf{X}_M - \mathbf{X}_N) \quad (7)$$

where  $\mathbf{X}_M, \mathbf{X}_N$  and  $\mathbf{x}_M$  denote the coordinates of the point  $N$  e  $M$  before and after the mapping, respectively.

**BOX 1 - First Derivative Recovery Algorithm**

- 1 - Define the *patch* associated to node  $N$
- 2 - Build the metric tensor  $\mathbf{S}(N)$ , from information about the mesh shape around of the node  $N$ , defined by the known parameters  $s(N)$ ,  $h(N)$ ,  $\mathbf{e}_1$  and  $\mathbf{e}_2$ .
- 3 - Transform all of the elements of the *patch*.
- 4 - Compute the gradients  $gradu_h$  in each one of the transformed elements.
- 5 - Using the recovering algorithm, compute  $grad_{Ru_h}(N)$ .
- 6 - By  $\nabla_{Ru_h}(N) = \mathbf{S}^T(N)grad_{Ru_h}(N)$  transform the gradient  $grad_{Ru_h}(N)$  to the original domain.

### 3. ADAPTIVE PROCEDURE

As mentioned before, it is taken as a local error indicator at element level,  $\eta_T$ , the value expressed by Eq.(4). Denoting  $\eta$  the global error indicator in the triangulation  $\mathfrak{S}_k$ , given by Eq.(5), the main idea to adapt the mesh, according to this error indicator, is to find a new mesh  $\mathfrak{S}_{k+1}$ , with a given number of elements  $Nel$ . The new finite element mesh is generated trying to produce a uniform distribution of the local error estimator over all elements.

As already said, our remeshing algorithm is based on the *advancing front technique*. In this technique, the mesh generator tries to build equilateral triangles in the metric defined by the variable metric tensor  $\mathbf{S}$  which, at node  $N$  of the actual mesh, takes the value defined by Eq.(13). To evaluate the parameters we proceed as follows (see Feijóo *et al.* 1997, for more details).

1. For each element compute the local error  $\eta_T$  and then compute the global error  $\eta$
2. Given a number of elements  $Nel$  in the new adapted mesh, the expected local error indicator is given by

$$\eta^* = \frac{\eta}{\sqrt{Nel}} \quad (8)$$

3. The decreasing or increasing rate of the element size is estimated by

$$\beta_T = \left( \frac{\eta^*}{\eta_T} \right)^{\frac{1}{3}} \quad (9)$$

From the rate  $\beta_T$ , computed at element wise, different approaches can be selected to find the distribution at nodal level. Those approaches can be the same used to perform the derivatives. This rate at nodal level is noted  $\beta(N)$ .

4. The size of the new element, to be generated at node  $N$ , is  $h_{k+1}(N) = \beta(N)h_k(N)$ . Two threshold values for the computed new element size are used

$$\underline{\alpha} * h_k \leq h_{k+1} \leq \bar{\alpha} * h_k \leq L \quad (10)$$

These two parameters are used in order to ensure a progressively mesh adaptation to the solution. Moreover,  $L$  represents the characteristic length of the domain  $\Omega$ .

5. The stretching factor  $s$  at node  $N$  is defined by  $s(N_k) = \sqrt{|\lambda_2|/|\lambda_1|}$ , where  $|\lambda_1| \leq |\lambda_2|$  are the absolute eigenvalues of the Hessian matrix  $\mathbf{H}(u_h(N))$ . This stretching factor must be bounded in order to ensure that the length of the element in the direction  $\mathbf{e}_1$ ,  $sh_{k+1}$ , must be no greater than the characteristic length  $L$  of the domain  $\Omega$ , i.e.,  $s \leq L/h_{k+1}$ .
6.  $h_{k+1}$  – *scaling*. Due to the limitation on the values of  $h$  and  $s$  the number of elements in the new adapted mesh may be different from the expected  $Nel$ . To force the equality between these two numbers, the element size  $h$  at nodal level, must be scaled. In particular, the number of elements in the new finite element mesh and the scaled value for the element size are given by

$$Nel_{new} = \frac{4}{\sqrt{3}} \int_{\Omega} \frac{2}{sh^2} d\Omega \quad \text{and} \quad h_{k+1} \leftarrow \sqrt{\frac{Nel_{new}}{Nel}} \times h_{k+1} \quad (11)$$

The adaptive strategy described is repeated until the error estimator in the mesh  $\mathfrak{S}_k$ , relative to the solution of the problem analyzed, becomes lower than a given admissible relative error  $\bar{\gamma}$ .

#### 4. LIMIT ANALYSIS

Under the assumption of proportional loading, the limit analysis problem consists in finding a load factor  $\alpha$  such that the body undergoes plastic collapse when subject to the reference loads  $F$  uniformly amplified by  $\alpha$ . In turn, a system of loads produces plastic collapse if there exists a stress field in equilibrium with these loads, which is plastically admissible and related, by the constitutive equations, to a plastic strain rate field being kinematically admissible. Thus, the limit analysis problem consists in finding  $\alpha \in \mathfrak{R}$ , a stress field  $T \in W'$ , a plastic strain rate field  $D^p \in W$  and a velocity field  $v \in V$  such that

$$D^p = \mathcal{D}v, \quad v \in V \quad (12)$$

$$\int_{\mathcal{B}} T \cdot Dv \, d\mathcal{B} = \alpha \left\{ \int_{\mathcal{B}} b \cdot v \, d\mathcal{B} + \int_{\Gamma_{\tau}} \tau \cdot v \, d\Gamma \right\}, \quad \forall v \in V \quad (13)$$

$$T \in \mathbf{P} = \{T \in W' \mid f(T) \leq 0, \quad \forall x \in \mathcal{B}\} \quad (14)$$

$$D^p = \nabla f(T) \dot{\lambda} \quad (15)$$

$$f \cdot \dot{\lambda} = 0, \quad \dot{\lambda} \geq 0 \quad \text{and} \quad f \leq 0 \quad (16)$$

We explain, in what follows, the above notation and the meaning of these relations. Equation (12) imposes that the collapse plastic strain rate is related to a kinematically admissible velocity field  $v$  by means of the tangent deformation operator  $\mathcal{D}$ . The Principle of Virtual Power, Eq.(13), imposes the equilibrium of the stress fields with a given body loads  $\alpha b$  and surface loads  $\alpha \tau$  prescribed in region  $\Gamma_{\tau}$  of the body.

For elastic ideally-plastic materials the plastic admissibility of stress fields is defined by the set  $\mathbf{P}$ , as in Eq.(14). The admissibility function  $f$  is a  $m$ -vector field, comprising in

each component a plastic mode. The inequality in Eq.(14) is understood as imposing that each one of those components  $f_k$  is non-positive. The constitutive relation is expressed by the normality rule Eq.(15) and complementarity condition Eq.(16). In Equation (16),  $\nabla f(T)$  denotes the gradient of  $f$ , and  $\lambda$  is the  $m$ -vector field of plastic multipliers. Also, in Eq.(16) the inequalities hold component wise.

The discretized version of the limit analysis formulation leads to a finite dimensional problem that can be seen as a discrete version of the Eqs.(12-16). A Newton-like strategy for solving this discrete problem is described by Borges *et al.*, (1996).

### BOX 2 - Adaptive Strategy for Limit Analysis

**Repeat**

- 1 - Apply the Newton-like strategy for solving the discrete limit analysis.
- 2 - Choose the control variable and compute the local estimator error  $\eta_T$  and the global error  $\eta$
- 3 - For a given  $Nel$ , for each node of the mesh  $\mathfrak{S}_k$  estimate  $\eta^*$ ,  $h_{k+1}$  and  $s_{k+1}$ .
- 4 - Scale  $h_{k+1}$
- 5 - Generate a new mesh  $\mathfrak{S}_{k+1}$ .

**Until**  $\eta_k \leq \bar{\gamma}\{\|u_h\|_{L_2(\Omega)} + \eta_k\}^{\frac{1}{2}}$

The choice of a variable to be used to control the adaptive process is not obvious. To capture the discontinuities, the natural choice is one of the components of the velocity vector field, provided that we can estimate in advance which component is suitable to this aim. However, this is not an easy task for a general problem. Unlike the velocity field, the scalar field of plastic multipliers may be used as control variable without the previous disadvantage. Because we observe in Eq.(15), that  $\dot{\alpha}$  is positive only when the function  $f_k$  is zero, that is, when the stress is on the yield surface. So, the plastic multipliers clearly indicate the region where localized plastic deformations or slip bands are present. As a consequence, the local singularities arising from these localized plastic deformations are also detected in this way. Based on this argument, the scalar field of plastic multipliers appears to be a good choice as control variable and is adopted for the most of the applications.

## 5. NUMERICAL APPLICATIONS

This section is devoted to numerical applications using the proposed mesh adaptive strategy. Before we apply the adaptive procedure for Limit Analysis problems, we select a test case in order to analyze the performance of the proposed adaptive mesh refinement process. This comparison will be allow us to select the most appropriate recovery procedure for our particular application.

### 5.1. Test case

We adopt an initial coarse mesh with 25 nodes and 32 elements, as shown in Fig.1. As an approximation for the function analysed we adopt the finite element linear/quadratic interpolant  $u_h$ , defined in the triangle  $T \in \mathfrak{S}_k$ , i.e.  $u_h(x_N, y_N) = u(x_N, y_N)$ , where  $(x_N, y_N)$  are the coordinates of the nodal point  $N$  in the finite element mesh  $\mathfrak{S}_k$ . All the adaptive process was performed considering an expected number of elements in the new adapted

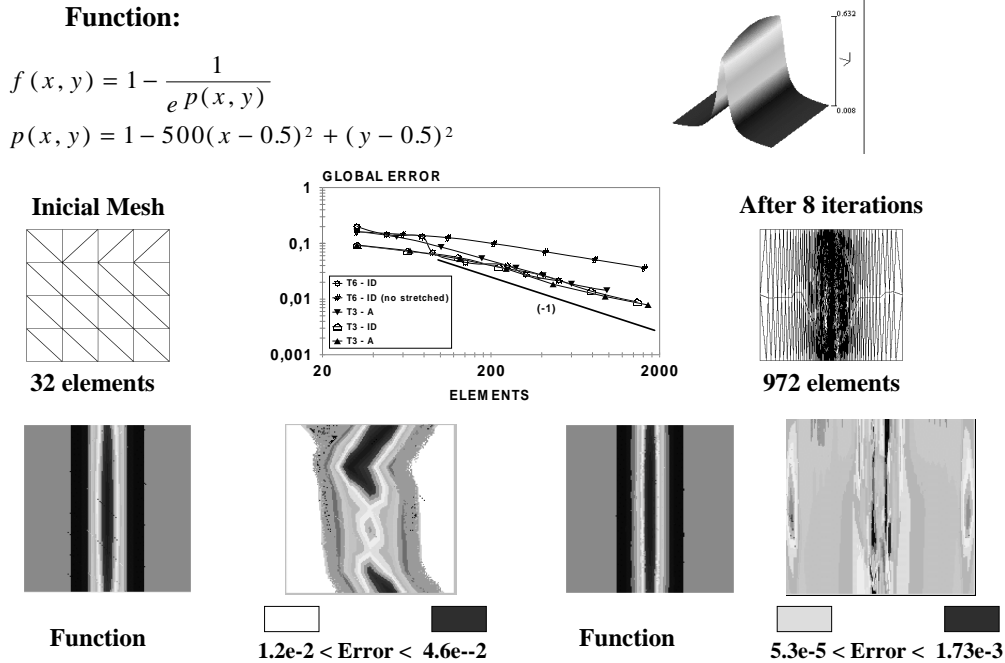


**Figure 1: Teste Function - T3/T6 - Linear/Quadratic Triangles  
ID/A - Inverse Distance/Area recovery procedure**

mesh ( $Nel$ ) twice the number of elements in the preceding one. The threshold values adopted for the new element size, as defined in Eq.(10), are  $L = 0.5$  and  $\underline{\alpha} = 0.05$ .

By using a graphic in  $\log \times \log$  scale, we present in the Fig.1 the global error  $\eta$  versus the total number of elements. We observe a good convergence rate for all the estimators plotted. The improvement in the convergence rate, by the adoption of stretched finite elements, becomes clear from the analysis of the plotted results.

In the same figure, we also present the mesh, the isovalues of the function and the distribution of the local error in the initial steps and after eight steps of adaptation. We can observe a fine homogeneity obtained in the error distribution.

## 5.2. Limit Analysis application - Frictionless extrusion through a square die.

We have simulated a plane strain frictionless extrusion with reduction of  $1/3$  and a Mises material. Because of the symmetry, we model only the upper half with the dimensions shown in Fig. 2. Lubliner,(1990), gives the exact solution  $p = 1.97900 \sigma_Y$  for the piston pressure at collapse. The analytical collapse mechanism presents localized deformation in the form of slip bands, as shown in the top of the figure.

As shown in Fig. 2, the plastic multiplier field, used as the control variable, is effective as a controller for the error estimator. The isovalues for the plastic deformation and local error show that the proposed procedure is also effective in capturing the localized plastic deformation. Indeed, it increases the nodal points of the mesh only near the region where the discontinuities take place, as well as it constructs elements which are aligned and stretched in the direction of slip bands.



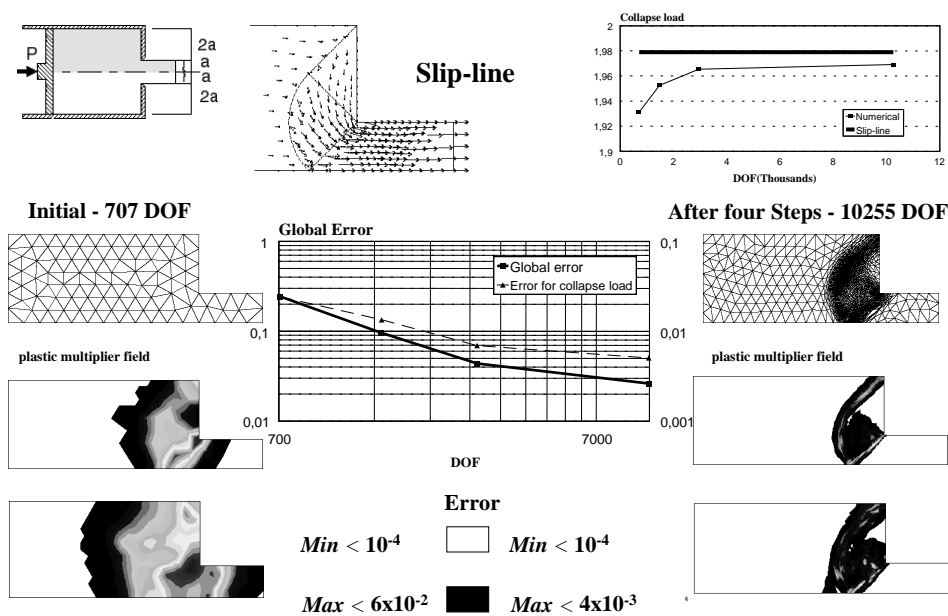


Figure 2: Frictionless extrusion through a square die.

## 6. CONCLUSION

The adaptive technique proposed shows to be appropriated to capture discontinuities arising from the localized plastic deformations during plastic collapse, and as a consequence, it deeply improves the numerical evaluation of the collapse load. The numerical applications confirmed the feasibility of process, that is, the computation of the error estimate was less expensive than the calculation of the numerical solution. In all studied cases the time spent in the adaptive strategy was lower than 1% of the total time spent in computing the solution of the problem.

### *Acknowledgement*

The authors would like to acknowledge the support of this research by their own institutions and by CNPq and CAPES. Also they are grateful to TACSOM group ([www.lncc.br/~tacsom](http://www.lncc.br/~tacsom)) by the softwares facilities offered.

## REFERENCES

- Almeida, R.C., Feijóo, R.A., Galeão, A.C.N., Padra, C. and Simões, R., 1998, Adaptive finite element computational fluid dynamics using an anisotropic error estimator, Computational Mechanics - New Trends and Applications, Fourth World Congress on Computational Mechanics - IV WCCM, Argentina.
- Borges, L.A, Feijóo, R.A., Padra, C. and Zouain, N., 1998, A Directional error estimator for adaptive finite element analysis, Computational Mechanics - New trends and

Applications - Fourth World Congress on Computational Mechanics - IV WCCM, Argentina.

Borges,L.A., Zouain N. and Huespe,A.E., 1996, A nonlinear optimization procedure for limit analysis, *European Journal of Mechanics A/Solids*, 15, n.3, 487-512.

Dompierre,J., Vallet,M.G., Fortin,M., Habashi,W.G., Aït-Ali-Yahia,D., Boivin,S., Bourgault,Y. and Tam,A., 1995, Edge-based mesh adaptation for CFD, *Conference on Numerical Methods for the Euler and Navier-Stokes Equations*, Montreal, 265-299.

Fancello,E., Guimarães,A.C.S. and Feijóo,R.A., 1990, ARANHA - Gerador de malhas 2D para elementos finitos triangulares de 3 e 6 nós, *Encuentro Nacional de Investigadores y Usuarios del Metodo de los Elementos Finitos*, Mar del Plata, Argentina, 05-09 de noviembre.

Feijóo,R.A., Borges,L. and Zouain,N., 1997, Estimadores *a posteriori* y sus aplicaciones en el análisis adaptativo, *International Report*, n.1/97, COPPE-UFRJ.

Lubliner, J., 1990, *Plasticity Theory*, Macmillan Publishing Company.

Peiró,J., 1989, A finite element procedure for the solution of the euler equations on the unstructured meshes, Ph.D. Thesis, Department of Civil Engineering, University of Swansea, UK.

Zienkiewicz,O.C. & Zhu,J.Z., 1992, The superconvergent patch recovery and a posteriori error estimates. Part 1 : The recovery technique, Part 2 : Error estimates and adaptivity, *Int. J. Numer. Methods Eng.*, 33, 1331-1382.